Global metric regularity of the devil's staircase of topological entropy

Ke-Fei Cao,[1,2,3] Zhong-Xuan Chen,[1] and Shou-Li Peng[1,2]
[1] *Center for Nonlinear Complex Systems, Department of Physics, and Institute of Applied Mathematics of Yunnan, Yunnan University, Kunming, Yunnan 650091, China*
[2] *China Center of Advanced Science and Technology (World Laboratory), P.O. Box 8730, Beijing 100080, China*
[3] *Department of Physiology and Centre for Nonlinear Studies, University of Leeds, Leeds LS2 9JT, United Kingdom*
(Received 23 August 1994)

In this paper, the global metric regularity of the devil's staircase of topological entropy is discussed by employing the quadratic map $f(x)=1-\lambda x^2$ as an actual metric model. The generalized dimensions, singularity spectra, "free energy," and the similarity between subintervals with an infinite number of scales in the entropy staircase are calculated. A lower bound 0.86 of chaotic measure in the entropy staircase is obtained.

PACS number(s): 05.45.+b, 03.20.+i, 05.20.Gg, 05.70.Jk

I. INTRODUCTION

We have shown [1] that the devil's staircase of topological entropy is an inevitable conclusion of topological classification of dynamic symbols (words). Because the devil's staircase reveals an algebraical structure (the Derrida-Gervois-Pomeau $*$ composition) of all admissible words in the topological space Σ_2 of two symbols, symbolic dynamics becomes a fundamental means for analyzing Σ_2 space. We also indicate that the devil's staircase is universal in interval dynamics because of the universality of Metropolis-Stein-Stein (MSS) sequences. However, there is still an important problem of the metric universality that needs to be resolved. The aim of this paper is to explore the global metric regularity of the devil's staircase. For convenience, the notations and their meanings in this paper are the same as in Ref. [1]. There, the following characteristics of the devil's staircase are proved by symbolic dynamics [1].

The zero-entropy interval

$$\Delta_F=\bigcup_{n=0}^{\infty} R^{*n}*[L^{\infty},R^{\infty}] \tag{1.1}$$

is located at the left in the h-λ space, and the nonzero-entropy interval is the union of subintervals Δ_n, $n=0,1,2,\ldots,$

$$[R^{*\infty},RL^{\infty}]=\bigcup_{n\in\mathbf{Z}^+}\Delta_n = \bigcup_{n\in\mathbf{Z}^+} R^{*n}*[RLR^{\infty},RL^{\infty}]\ ; \tag{1.2}$$

here $RLR^{\infty}=R*RL^{\infty}$ is the minimal limit of primitive words. The typical representative of the nonzero-entropy interval is the primitive word subinterval

$$\Delta_0=[RLR^{\infty},RL^{\infty}]\ , \tag{1.3}$$

which is located at the right in the space. The h versus λ curve in Δ_0 includes an infinite number of equal topological entropy class (ETEC) steps. The step corresponding to the primitive word $\mathbf{Q}_i\in\mathcal{P}_\pi$ ($\mathcal{P}_\pi$ means the set of all primitive words) is

$$H_{\mathbf{Q}_i}=\mathbf{Q}_i*[L^{\infty},RL^{\infty}],\quad i=1,2,\ldots\ . \tag{1.4}$$

Outside steps on the h versus λ curve in Δ_0 there are an infinite number of isolated single points, which correspond to infinitely long aperiodic sequences and represent either fine-grain or coarse-grain chaos under a finite resolution. The h versus λ curve in Δ_0 possesses a multifractal structure. This multifractal curve is successively compressed and made to fill the subintervals $\Delta_1,\Delta_2,\ldots,$ up to the zero-entropy interval Δ_F, by $R^{*n}*$ ($n=1,2,\ldots,\infty$). These multifractal curves are similar because of the uniform compressibility of $R*$, and combine to form the complete devil's staircase of topological entropy.

As contrasted with theoretical work, calculating work on a map is very time consuming because of the enormous number of primitive words. For example, in the unimodel map

$$f(x,\lambda)=1-\lambda x^2,\quad x\in(-1,+1),\quad \lambda\in(0,2)\ , \tag{1.5}$$

we spent more than 1000 h of CPU time on a VAX-8350 computer calculating about 5×10^3 sequences. Therefore we can only use (1.5) as an actual example to discuss the global metric regularity of the devil's staircase and calculate its thermodynamic functions. In Sec. II, we first metrize the kneading sequence space, and calculate the Lebesgue measure of ETEC steps. In Sec. III, we discuss the multifractal structure with an infinite number of scales of the primitive word subinterval Δ_0, and calculate its generalized dimensions, singularity spectra, and "free energy." In Sec. IV, we show the quantitative relation of similarity between nonprimitive word subinterval Δ_n ($n=1,2,\ldots$) and primitive word subinterval Δ_0. Finally, in Sec. V, from the above we derive the global metric regularity of the topological entropy curve, and obtain the lower bound of the chaotic measure in the entropy staircase.

 ©1995 The American Physical Society

II. THE LEBESGUE MEASURE OF THE ETEC STEPS

A. The metrization of the kneading sequence space

It is a convenient and natural method of metrization to take the value of parameter of a kneading sequence as its metric. For the superstable periodic kneading sequence $\mathbf{W}C$, the value of parameter $\lambda_{\mathbf{W}}$ can easily be calculated with the word-lifting technique [2]. Corresponding to $\mathbf{W}C$, there is a periodic window [3] $\mathbf{W}L^{t(\mathbf{W})} < \mathbf{W}C < \mathbf{W}R^{t(\mathbf{W})}$, which has period $(\|\mathbf{W}\|+1)$. For given $\mathbf{W}$, the values of parameter λs (and periodic points x_i) corresponding to the lower sequence $\mathbf{W}L^{t(\mathbf{W})}$ and the upper sequence $\mathbf{W}R^{t(\mathbf{W})}$ can be found, respectively, while solving by Newton's method the systems of equations of the fixed points and the boundary condition as follows:

$$f^k(x,\lambda)=x \ , \qquad \left|\prod_{i=1}^{k} f'(x_i,\lambda)\right|=1 \ . \tag{2.1}$$

The mapping function f should be replaced by f^{-1} in practice so as to determine the unique solution of the parameter λ using the symbolic sequence of either $\mathbf{W}L^{t(\mathbf{W})}$ or $\mathbf{W}R^{t(\mathbf{W})}$.

It is not difficult to metrize an aperiodic sequence. For the Zheng-Hao type of sequence $\rho\lambda^{\infty}$, their values of the parameter can be determined by the generalized word-lifting technique [2]. For an infinite aperiodic sequence, its systems of equations (2.1) can be written formally. In actual calculation, however, an aperiodic sequence has to be truncated and made into a sufficiently long symbolic sequence so as to approach its value of the parameter.

As mentioned above, for a unimodel map, an amdissible sequence $\mathbf{W}\in\mathcal{W}$ (the letter C in sequence $\mathbf{W}C$ is absorbed hereafter, and $\mathcal{W}$ means the set of all admissible sequences) must have a corresponding value of parameter $\lambda_{\mathbf{W}}$, and vice versa. Thus the number of admissible sequences is as large as the number of real numbers in [0,1], all admissible sequences are consecutive, and $\mathcal{W}$ possesses the cardinal number of the continuum. In other words, an additional admissible sequence can be inserted between any two admissible sequences, and this can be repeated *ad infinitum*. This property of the topological symbolic sequences exhibits continuity in parametric metric space:

$$\lim_{\mathbf{W}_1\to\mathbf{W}_2}\lambda_{\mathbf{W}_1}=\lambda_{\mathbf{W}_2} \ . \tag{2.2}$$

The order in topological space (MSS order) is consistent with the order in parameter space, namely, if $\mathbf{W}_1<\mathbf{W}_2$, then $\lambda_{\mathbf{W}_1}<\lambda_{\mathbf{W}_2}$. Therefore we can naturally introduce the parametric metric of the subset $[\mathbf{W}_1,\mathbf{W}_2]([\mathbf{W}_1,\mathbf{W}_2]$ means the minimal sequence is $\mathbf{W}_1$ and the maximal sequences $\mathbf{W}_2$ in the sequence set)

$$|[\mathbf{W}_1,\mathbf{W}_2]|=\lambda_{\mathbf{W}_2}-\lambda_{\mathbf{W}_1} \ . \tag{2.3}$$

Obviously, the parametric metric $|\ |$ preserves the isomorphism between the MSS order and the parameter order.

B. Calculating the width of an ETEC step

Noting the compressibility of $\mathbf{W}*$, $\mathbf{W}\in\mathcal{W}=[L^{\infty},RL^{\infty}]$, we have

$$|\mathbf{W}*[L^{\infty},RL^{\infty}]|<|[L^{\infty},RL^{\infty}]| \ . \tag{2.4}$$

Since the topological entropy of a compound kneading sequence is [1]

$$h(\mathbf{Q}*\mathbf{S})=\begin{cases} h(\mathbf{Q}) & \text{if } \mathbf{Q}\neq R^{*n} \ , \\ \dfrac{1}{2^n}h(\mathbf{S}) & \text{if } (\mathbf{Q})=R^{*n} \ , \end{cases} \tag{2.5}$$

and taking $\mathbf{W}$ as a primitive word $\mathbf{Q}$, we obtain the ETEC step $H_{\mathbf{Q}}$,

$$H_{\mathbf{Q}}=\mathbf{Q}*[L^{\infty},RL^{\infty}], \quad \mathbf{Q}\in\mathcal{P}_{\pi} \ . \tag{2.6}$$

Obviously, $H_{\mathbf{Q}}$ is a compact closed set, possesses the cardinal number of the continuum, and occupies the Lebesgue measure in the parameter space. After metrizing the ETEC, the width of step $H_{\mathbf{Q}}$ is

$$\Lambda_{h(\mathbf{Q})}=|\mathbf{Q}*[L^{\infty},RL^{\infty}]|=|[\mathbf{Q}L^{t(\mathbf{Q})},\mathbf{Q}*RL^{\infty}]| \ . \tag{2.7}$$

This formula indicates that the left terminal of step $H_{\mathbf{Q}}$ corresponds to the value of the parameter of the lower sequence, and the right terminal to that of $\mathbf{Q}*RL^{\infty}$. In actual calculation, RL^{∞} must be truncated and made into the sequence RL^{n-2} with period n. We found that a high precision ($\sim 10^{-32}$) is reached when taking $n=100$.

In numerical calculation of the quadratic map $f(x)=1-\lambda x^2$ the results indicate that the word RLC with period 3 has the maximal width

$$\max\{\Lambda_{h(\mathbf{Q})}\}=\Lambda_{h(RL)}=0.0403\ldots \ , \tag{2.8}$$

and that among various primitive words with the same period $\|\mathbf{Q}\|$ there is an approximate relation

$$\min\{\Lambda_{h(\mathbf{Q})}\}\sim\Lambda_{h(RL^{\|\mathbf{Q}\|-2})}\sim 10^{-\|\mathbf{Q}\|} \ ,$$

which implies other facts related to the global regularities.

III. THE METRIC PROPERTIES OF THE ENTROPY STAIRCASE IN THE PRIMITIVE WORD SUBINTERVAL

The method described in Sec. II enables us to calculate the multifractal property of the entropy staircase and establish its thermodynamic formalism, i.e., calculate its generalized dimension D_q, singularity spectrum $f(\alpha)$, and free energy. We first calculate these quantities in the primitive word subinterval Δ_0.

A. The complementary set Δ_0^C and its support $\Delta_{0,k}^C$

In Δ_0 there are an infinite number of ETEC steps $H_{\mathbf{Q}_i}$ [1], the width of which is given by

$$\Lambda_{h(\mathbf{Q}_i)}=|\mathbf{Q}_i*[L^{\infty},RL^{\infty}]|, \quad \mathbf{Q}_i\in\mathcal{P}_{\pi} \ . \tag{3.1}$$

Taking the width of the subinterval Δ_0

$$|\Delta_0| = |[RLR^{\infty}, RL^{\infty}]| \tag{3.2}$$

as the normalized width, each $\Lambda_{h(Q_i)}$ can be rescaled. Thus the h versus λ curve in Δ_0 is a multifractal curve [1] with an infinite number of scales

$$\gamma_i = \frac{\Lambda_{h(Q_i)}}{|\Delta_0|}, \quad Q_i \in \mathcal{P}_\pi . \tag{3.3}$$

The complementary set Δ_0^C to the steps in the subinterval Δ_0 is defined as

$$\Delta_0^C = \Delta_0 \setminus \bigcup_{Q_i \in \mathcal{P}_\pi} Q_i * [L^{\infty}, RL^{\infty}] . \tag{3.4}$$

Since Δ_0^C contains all the aperiodic sequences, including all fine-grain and coarse-grain chaotic sequences under a finite resolution, it forms a chaotic set. This chaotic set possesses a very large Lebesgue measure $L(\Delta_0^C)$ [4], which distinguishes the entropy devil's staircase from the Jensen-Bak-Bohr devil's staircase in the mode-locking structure for the circle map, where the chaotic set only has a zero Lebesgue measure [5].

Denoting the number of all primitive words (i.e., steps in Δ_0) with period $3-k$ by N_k, the complementary set to the ETEC steps with period $3-k$ is

$$\Delta_{0,k}^C = \Delta_0 \setminus \bigcup_{i=1}^{N_k} Q_i * [L^{\infty}, RL^{\infty}], \quad Q_i \in \mathcal{P}_\pi, \quad 3 \le \|Q_i\| \le k , \tag{3.5}$$

which is the support of Δ_0^C and can be covered with $N_k^C = N_k + 1$ subintervals in the λ axis. Denoting the width of these coverings rescaled by the normalized width $|\Delta_0|$ by $l_1, l_2, \ldots, l_{N_k+1}$, which are the multiscale of the $\Delta_{0,k}^C$, thus for finite N_k^C,

$$0 < \sum_{i=1}^{N_k^C} l_i < 1, \quad 0 < l_i, \quad i = 1, 2, \ldots, N_k^C \tag{3.6}$$

and

$$\lim_{k \to \infty} \Delta_{0,k}^C = \Delta_0^C .$$

B. The generalized dimension D_q and singularity spectrum $f(\alpha)$

There are two methods for calculating the generalized dimension D_q and singularity spectrum $f(\alpha)$ of the chaotic set $\Delta_{0,k}^C$.

1. The Halsey method

This is an indirect method which determines D_q by Newton's method from the following sum rule [6]:

$$\sum_{i=1}^{N_k^C} \frac{p_i^q}{l_i^\tau} = 1 , \tag{3.7}$$

where $\tau = (q-1)D_q$, p_i is the probability corresponding to the ith covering with normalized width scale l_i, and $p_i = 1/N_k^C = 1/(N_k+1)$, if the homogeneity of the chaotic set is taken for granted. In practice, when our calculation went as far as $k = 16$ ($N_k = 4338$), satisfactory results were obtained. We have

$$D_q(\Delta_0^C) \approx D_q(\Delta_{0,16}^C) . \tag{3.8}$$

When $q = 1$, the formula (3.7) becomes invalid. The value of D_1 can be calculated directly from the formula

$$D_1 = \frac{\sum_{i=1}^{N_k^C} p_i \ln p_i}{\sum_i p_i \ln l_i} = -\frac{N_k^C \ln N_k^C}{\sum_i \ln l_i} . \tag{3.9}$$

Table I gives the numerical results for D_0 and D_1 in the computer experiment of the quadratic map $f(x) = 1 - \lambda x^2$. The curve D_q versus q ($-30 \le q \le 30$) is drawn in Fig. 1. The singularity spectrum $f(\alpha)$ can be found from D_q according to the Legendre transformation

$$f(\alpha) = q\alpha - \tau , \tag{3.10}$$

where $\alpha = d\tau/dq$. The result is drawn in Fig. 2 (dashed line).

TABLE I. The value of D_0 and D_1 in the map $f(x) = 1 - \lambda x^2$ (by the Halsey method).

k	N_k^C	D_0	D_1
3–11	196	0.9706	0.8378
3–12	355	0.9730	0.8352
3–13	670	0.9756	0.8406
3–14	1237	0.9773	0.8397
3–15	2322	0.9790	0.8423
3–16	4339	0.9804	0.8430

2. The Chhabra-Jensen method

There are many elements in the support $\Delta_{0,k}^C$. Using "boxes" of size l to cover the members of $\Delta_{0,k}^C$, and denoting the probability in the ith "box" by $p_i(l)$, we have

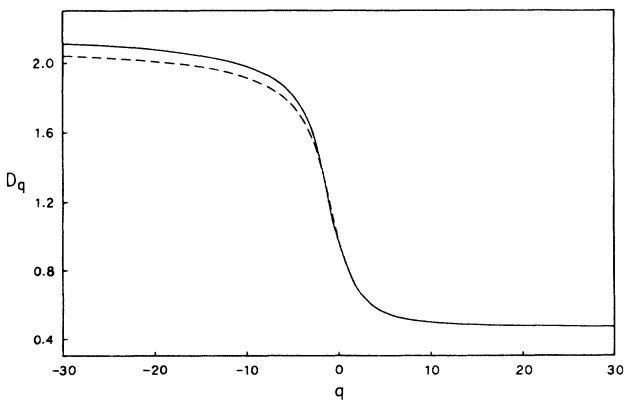

FIG. 1. The curves D_q vs q in Δ_0^C. The solid line is by the Chhabra-Jensen method; the dashed by the Halsey method.

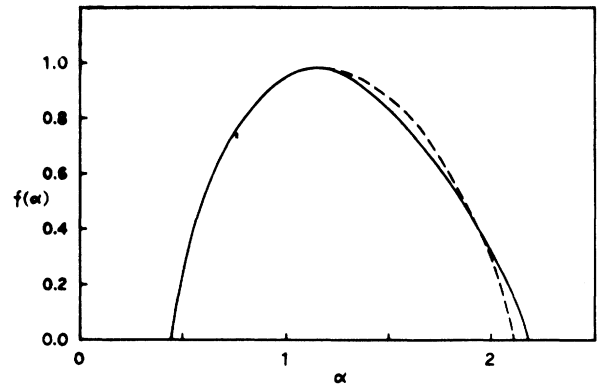

FIG. 2. The singularity spectrum of Δ_0^C in the map $f(x)=1-\lambda x^2$ by the two methods.

$$D_q=\lim_{l\to 0}\frac{1}{q-1}\frac{\ln\sum_i p_i^q(l)}{\ln l}, \tag{3.11}$$

$$D_1=\lim_{l\to 0}\frac{\sum_i p_i(l)\ln p_i(l)}{\ln l}. \tag{3.12}$$

According to Chhabra and Jensen [7], in actual calculation we need not take the limit $l\to 0$ but take the mean of l,s as l,

$$l=\frac{\sum_{i=1}^{N_k^C} l_i}{N_k^C}. \tag{3.13}$$

Then the probability reads

$$p_i(l)=\frac{l_i}{\sum_j l_j}. \tag{3.14}$$

Obviously, $\sum_i p_i=1$.

While calculating the singularity spectrum $f(\alpha)$, instead of the Legendre transformation, we may construct a family of single parameters with the normalized measure

$$\mu_i(q,l)=\frac{p_i^q(l)}{\sum_j p_j^q(l)}, \tag{3.15}$$

and directly compute the singularity spectrum

$$f(q)=\lim_{l\to 0}\frac{\sum_i \mu_i(q,l)\ln\mu_i(q,l)}{\ln l}. \tag{3.16}$$

The mean of the singularity is

$$\alpha(q)=\lim_{l\to 0}\frac{\sum_i \mu_i(q,l)\ln p_i(l)}{\ln l}. \tag{3.17}$$

When $q=1$, $\mu_i(1,l)=p_i(l)$, we have

$$f(\alpha(1))=\alpha(1)=D_1. \tag{3.18}$$

The results are exhibited in Fig. 2 (solid line). Some numerical values of D_q of special meaning are given in Table II.

Both methods give consistent results. The comparisons between curves of D_q-q and $f(\alpha)$-α are also shown in Figs. 1 and 2, respectively. Nearly identical numerical results for D_0 (~ 0.98) are obtained by these two methods. Theoretically, however, D_0 should be 1 because $L(\Delta_0^C)>0$. It is easily found from formulas (3.6), (3.13), (3.14), and (3.11) (taking $q=0$) that

$$D_0=\frac{\ln N_k^C}{\ln N_k^C+\left|\ln\sum_i l_i\right|}<1. \tag{3.19}$$

Since N_k^C is a finite number, $D_0<1$ is inevitably obtained by the Chhabra-Jensen method. On the other hand, by the Halsey method, the result $D_0<1$ is also obtained because

$$0<\sum_{i=1}^{N_k^C} l_i<1,\quad \sum_{i=1}^{N_k^C} l_i^{D_0}=1. \tag{3.20}$$

Therefore the fact that the numerical result $D_0<1$ is obtained is not due to the limitations of the computer, but the impossibility of carrying on the calculation indefinitely. From (3.19), it is seen that while $N_k^C\to\infty$, $D_0\to 1$. We believe that $D_0\approx 0.98$ is a good approximation to the theoretical value. We will only use the results of the Chhabra-Jensen method hereafter.

C. The free energy in the chaotic set Δ_0^C

According to Feigenbaum [8] the thermodynamic functions D_q and τ belong to the microcanonical ensemble for the system of dimension in the chaotic set Δ_0^C. They can be transferred to the canonical ensemble by free energy $F(\beta)$ which is defined asymptotically as

$$(N_k^C)^{-F(\beta)}=\sum_{i=1}^{N_k^C} l_i^\beta, \tag{3.21}$$

if $N_k^C\to\infty$, $F(\beta)$ becomes independent of N_k^C. The relation of the microcanonical ensemble functions to the canonical ensemble quantities is as follows:

TABLE II. Some special values of D_q.

Method	$D_0=f(\alpha(0))$	$D_1=f(\alpha(1))=\alpha(1)$	$D_{-\infty}=\alpha_{\max}$	$D_{+\infty}=\alpha_{\min}$
Halsey	0.9804	0.8430	2.109	
Chhabra-Jensen	0.9837	0.8138	2.180	0.450

$$q=-F(\beta),\quad \tau=(q-1)D_q=-\beta\ . \tag{3.22}$$

Thus, the free energy $F(\beta)$ in the chaotic set Δ_0^C is

$$F(\beta)=\beta/D_q-1\ . \tag{3.23}$$

The curve $F(\beta)$ versus β in Δ_0^C is shown in Fig. 3, and approaches a broken line formed by the following two lines:

$$\lim_{q\to+\infty}F(\beta)=\frac{1}{D_\infty}\beta-1\approx 2.20\beta-1\ , \tag{3.24}$$

$$\lim_{q\to-\infty}F(\beta)=\frac{1}{D_{-\infty,0}}\beta-1\approx 0.45\beta-1\ . \tag{3.25}$$

IV. THE METRIC PROPERTIES OF THE ENTROPY STAIRCASE IN THE NONPRIMITIVE WORD SUBINTERVAL

From the expression of the nonprimitive word subinterval

$$\Delta_n=R^{*n}*[RLR^\infty,RL^\infty],\quad n=1,2,\ldots, \tag{4.1}$$

and the formula of the topological entropy

$$h(R^{*n}*\mathbf{S})=\frac{1}{2^n}h(\mathbf{S})\ , \tag{4.2}$$

it is easily seen that the topological entropy decreases by a factor of $\frac{1}{2}$ as Δ_n changes to Δ_{n+1}. On the other hand, because of the compressibility of $R*$ the width of a subinterval should decrease by a factor of δ from Δ_n to Δ_{n+1}. In actual calculation of the quadratic map $f(x)=1-\lambda x^2$, taking $\mathbf{Q}_i$ over 4338 primitive words with periods 3–16, we found that

$$\lim_{n\to\infty}\frac{\Lambda_{h(R^{*n}*Q_i)}}{\Lambda_{h(R^{*(n+1)}*Q_i)}}=\lim_{n\to\infty}\frac{|\Delta_n|}{|\Delta_{n+1}|}=\delta(R)=4.6692\ldots\ . \tag{4.3}$$

Thus there is similarity between the subintervals

$$\Delta_0\sim\Delta_1\sim\cdots\sim\Delta_n\sim\Delta_{n+1}\sim\cdots,\quad n=0,1,2,\ldots\ . \tag{4.4}$$

Since there is the multifractal property in Δ_0, it is obvious due to the above-mentioned similarity that there is also the multifractal property in each nonprimitive word subinterval Δ_n, $n=1,2,\ldots$. Moreover, we can anticipate that

$$D_0(\Delta_0^C)=D_0(\Delta_1^C)=D_0(\Delta_2^C)=\cdots=D_0(\Delta_n^C),\quad n\in\mathbb{Z}^+\ . \tag{4.5}$$

By the Lipschitz transformation theorem [9], if $G\in\mathbb{R}^n$, map $g:G\to\mathbb{R}^n$ satisfies the conditions

$$C_1|u-v|\le|g(u)-g(v)|\le C_2|u-v|\ ,$$

$$u,v\in G\ \text{ and }\ 0<C_1\le C_2<\infty\ ;$$

then $D_0(g(G))=D_0(G)$. Taking g to be the compression map $R*$, employing the parametric metric in Sec. II, for any two words $\mathbf{Q}_1<\mathbf{Q}_2$, $\mathbf{Q}_1,\mathbf{Q}_2\in\Delta_0$, the following inequality holds:

$$C_1|[\mathbf{Q}_1,\mathbf{Q}_2]|\le|[R*\mathbf{Q}_1,R*\mathbf{Q}_2]|\le C_2|[\mathbf{Q}_1,\mathbf{Q}_2]|\ , \tag{4.6}$$

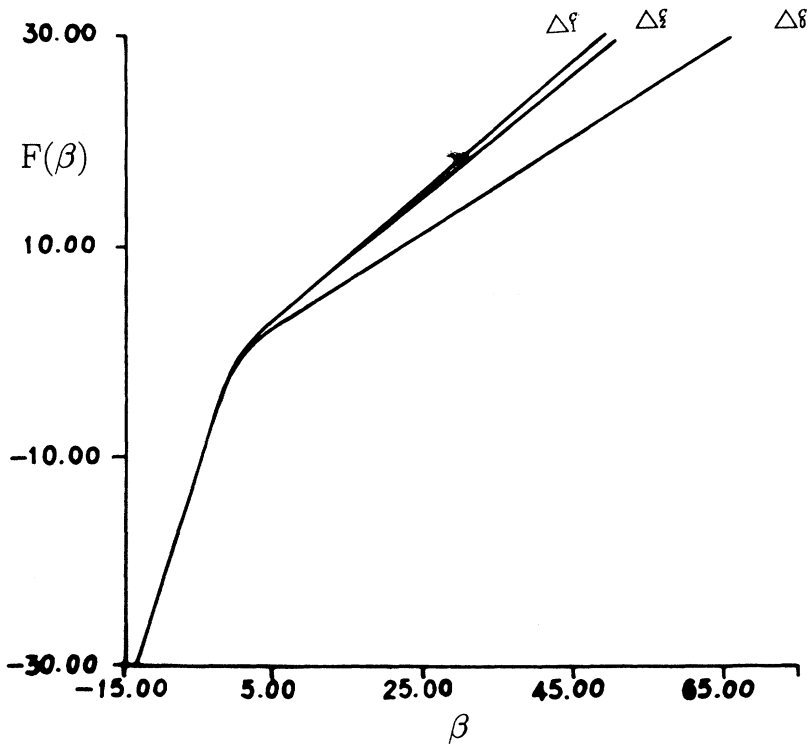

FIG. 3. The free energy curves $F(\beta)$ vs β in Δ_0^C, Δ_1^C, and Δ_2^C by the Chhabra-Jensen method.

TABLE III. The numerical results for D_0, D_1, $D_{-\infty}$, and $D_{+\infty}$.

Interval	Halsey method		Chhabra-Jensen method			
	D_0	D_1	D_0	D_1	$D_{-\infty}=\alpha_{\max}$	$D_{+\infty}=\alpha_{\min}$
Δ_0^C	0.9804	0.8430	0.9837	0.8138	2.1800	0.4500
Δ_1^C	0.9792	0.8791	0.9821	0.8401	1.6413	0.4480
Δ_2^C	0.9792	0.8730	0.9822	0.8339	1.7207	0.4468

where the constants C_1 and C_2 are chosen in the neighborhood of the Feigenbaum constant $\delta(R)$. We then have formula (4.5). This conclusion is verified by 3×4338 numerical data on the quadratic map, as shown in Table III and Fig. 4. It is seen in Fig. 4 that the curves D_q versus q ($n=0,1,2,$) merge when $q\geq0$ and separate when $q<0$. That is to say, the formula (4.5) still holds when $q>0$:

$$D_q(\Delta_0^C)=D_q(\Delta_1^C)=D_q(\Delta_2^C)=\cdots=D_q(\Delta_n^C),\quad n\in\mathbb{Z}^+ . \tag{4.7}$$

This fact indicates that the relation of similarity (4.4) between the subintervals is useful only when $q\geq0$. This is helpful to our understanding of the meaning of the generalized dimensions D_q of $q<0$.

Correspondingly, the curves $f(\alpha)$ versus α ($n=0,1,2$) in Fig. 5 merge when α values are small and separate when α values are large. It is seen in Fig. 5 that the curves $f(\alpha)$ versus α are different in width, even though they are the same in height ($D_0=1$). Therefore the singularity spectrum $f(\alpha)$ at large α is important for describing the multifractal structure of the entropy staircase.

Similarly, the broken lines $F(\beta)$ versus $\beta(n=0,1,2)$ in Fig. 3 merge when $\beta<0$, i.e., the line (3.24), and separate when $\beta>0$. When $n=1,2$, we have

$$\lim_{q\to-\infty}F(\beta)=\frac{1}{D_{-\infty,1}}\beta-1\approx0.61\beta-1 , \tag{4.8}$$

$$\lim_{q\to-\infty}F(\beta)=\frac{1}{D_{-\infty,2}}\beta-1\approx0.58\beta-1 . \tag{4.9}$$

It is an important result that the curves $F(\beta)$ versus β are linear in limiting cases.

V. THE GLOBAL METRIC REGULARITY OF THE DEVIL'S STAIRCASE OF TOPOLOGICAL ENTROPY

Summing up the discussion on subintervals Δ_n, $n=0,1,2,\ldots,$ of which the complete devil's staircase of topological entropy consists, the following conclusions about the global metric regularity of the devil's staircase of topological entropy are reached from our numerical calculation.

(1) When $q\geq0$, each subinterval Δ_n, $n=1,2,\ldots,$ possesses a similar structure to that of Δ_0. The generalized dimension of the complementary set of the complete entropy devil's staircase should be equal to the generalized dimension of the complementary set of any subinterval:

$$D_q(\Delta^C)\equiv D_q\left[\bigcup_{n\in\mathbb{Z}^+}\Delta_n^C\right]=D_q(\Delta_n^C),\quad q\geq0 , \tag{5.1}$$

$$D_0(\Delta^C)\equiv D_0\left[\bigcup_{n\in\mathbb{Z}^+}\Delta_n^C\right]=1 . \tag{5.2}$$

When $q<0$, the curves D_q-q in subintervals Δ_0, Δ_1, and Δ_2 will separate by the numerical calculation. It is an interesting problem to rescale these curves so that they may merge.

(2) The complementary set to the steps in each subinterval Δ_n, $n=0,1,2,\ldots,$ is a chaotic set. Because a ETEC step still contains a coarse-grain chaotic set such as $\mathbf{Q}_i*\mathcal{P}_{\text{chaos}}$ ($\mathcal{P}_{\text{chaos}}$ means the set of all chaotic sequences), only the lower bound of the normalized Lebes-

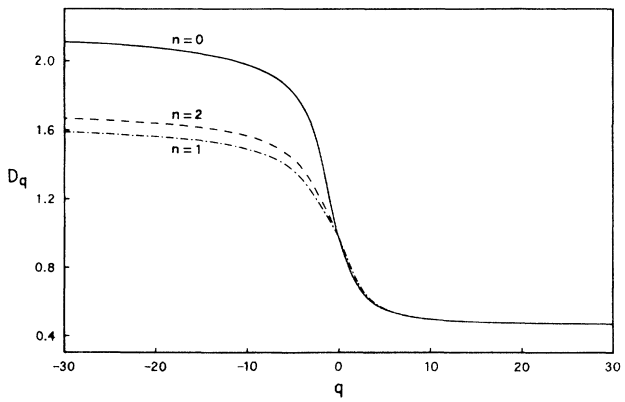

FIG. 4. The comparison between the curves D_q vs q in Δ_0^C, Δ_1^C, and Δ_2^C by the Chhabra-Jensen method.

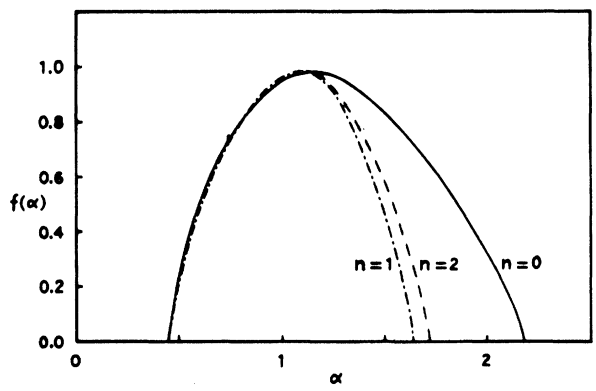

FIG. 5. The comparison between the singularity spectra of Δ_0^C, Δ_1^C, and Δ_2^C by the Chhabra-Jensen method.

TABLE IV. The normalized Lebesgue measure of N_k^* steps with the same period k in Δ_0.

k	N_k^*	$\sum_i \Lambda_{h(Q_i)}/\lvert\Delta_0\rvert$
3	1	
4	1	
5	3	0.023 748
6	3	0.000 772
7	9	0.006 571
8	13	0.001 545
9	27	0.001 948
10	45	0.000 396
11	93	0.000 827
12	159	0.000 287
13	315	0.000 301
14	567	0.000 143
15	1085	0.000 102
16	2017	0.000 073

gue measure of each complementary set

$$L(\Delta_n^C)=1-\sum_{Q_i\in\mathcal{P}_\pi}\Lambda_{h(R^{*n}*Q_i)}/\lvert\Delta_n\rvert \tag{5.3}$$

can be obtained. The normalized Lebesgue measures occupied by steps of primitive words with the same period in the subinterval Δ_0 are given in Table IV. From the table, it is seen that as the period k increases the number of primitive words under consideration increases sharply. However, the normalized Lebesgue measures occupied by steps of primitive words with a high period are very small. Thus an approximate lower bound of the chaotic measure can be obtained by the truncation method. The numerical results of $L(\Delta_{0,k}^C)$ are shown in Table V. The mean of the lower bound of the chaotic measure in the entropy staircase is

TABLE V. The numerical results of $L(\Delta_{0,k}^C)$.

k	N_k^C	$L(\Delta_{0,k}^C)$
3–4	3	0.906 777
3–5	6	0.883 029
3–6	9	0.882 256
3–7	18	0.875 686
3–8	31	0.874 141
3–9	58	0.872 193
3–10	103	0.871 797
3–11	196	0.870 970
3–12	355	0.870 682
3–13	670	0.870 382
3–14	1237	0.870 239
3–15	2322	0.870 137
3–16	4339	0.870 064

$$L(\Delta^C)\equiv L\left[\bigcup_{n\in Z^+}\Delta_n^C\right]=0.86\ . \tag{5.4}$$

(3) In the above numerical calculation, the quadratic map $f(x)=1-\lambda x^2$ is employed as an actual example. In other maps of quadratic maximum, such as $f(x)=\lambda' x(1-x)$ and $f(x)=\lambda''\sin\pi x$, the lower bounds should also be around 0.86 even though the widths of the steps in different maps may change. In the case of the map of z-order maximum $f(x)=1-\lambda|x|^z$, the structure of the entropy devil's staircase is still the same, but its global metric properties, such as D_q, $f(\alpha)$, and $L(\Delta^C)$, will change. This will be discussed elsewhere.

ACKNOWLEDGMENTS

This work is supported in part by the National Basic Research Project (Nonlinear Science) of China, the National Natural Science Foundation of China, and the Natural Science Foundation of Yunnan Provincial Education Commission.

[1] Z.-X. Chen, K.-F. Cao, and S.-L. Peng, preceding paper, Phys. Rev. E **51**, 1983 (1995).

[2] B.-L. Hao, *Elementary Symbolic Dynamics and Chaos in Dissipative Systems* (World Scientific, Singapore, 1989), pp. 105, 156.

[3] W.-M. Zheng, Report No. ASITP-88-006, 1988 (unpublished).

[4] P. Martin-Löf, Inf. Control **9**, 602 (1966); M. V. Jakobson, Commun. Math. Phys. **81**, 39 (1981); Y.-Q. Wang and S.-G. Chen, Acta Phys. Sin. **33**, 341 (1984).

[5] M. H. Jensen, P. Bak, and T. Bohr, Phys. Rev. Lett. **50**, 1637 (1983); P. Cvitanović, M. H. Jensen, L. P. Kadanoff, and I. Procaccia, *ibid.* **55**, 343 (1985).

[6] T. C. Halsey, M. H. Jensen, L. P. Kadanoff, I. Procaccia, and B. I. Shraiman, Phys. Rev. A **33**, 1141 (1986); **34**, 1601 (1986).

[7] A. Chhabra and R. V. Jensen, Phys. Rev. Lett. **62**, 1327 (1989); A. B. Chhabra, R. V. Jensen, and K. R. Sreenivasan, Phys. Rev. A **40**, 4593 (1989); A. B. Chhabra, C. Meneveau, R. V. Jensen, and K. R. Sreenivasan, Phys. Rev. A **40**, 5284 (1989).

[8] M. J. Feigenbaum, J. Stat. Phys. **46**, 919 (1987).

[9] K. J. Falconer, *Fractal Geometry, Mathematical Foundations and Applications* (Wiley, New York, 1990), Chap. 2.